J. Fluid Mech. (2012), *vol.* 706, *pp.* 58–70.
doi:10.1017/jfm.2012.211

Stability of biomimetic membranes in DC electric fields

Jacopo Seiwert[1], Michael J. Miksis[2] and Petia M. Vlahovska[1]†

[1] School of Engineering, Brown University, Providence, RI 02912, USA

[2] Department of Engineering Sciences and Applied Mathematics, Northwestern University, Evanston, IL 60202, USA

(Received 27 January 2012; revised 31 March 2012; accepted 26 April 2012; first published online 12 July 2012)

The interface defining a biological cell is a thin membrane, which acts as a leaky capacitor. We investigate the influence of capacitance and conductivity on the stability of a planar membrane subjected to a DC electric field. We develop a zero-thickness model of the membrane, in which the bilayer finite thickness is effectively accounted for by membrane electro-mechanical properties such as bending modulus, capacitance and conductance. The linear stability analysis shows that membrane conductance and asymmetry in the embedding electrolyte solutions destabilize the interface. However, the capacitive charging acts to stabilize the system under conditions where an ordinary fluid–fluid interface is unstable.

Key words: electrohydrodynamic effects, membranes

1. Introduction

Biological cells are enveloped by a nanometre-thick membrane, whose integrity is central to maintaining life. The cell membrane regulates the transport of substances between the cell interior and the extracellular space. To deliver exogenous molecules (such as drugs and DNA) into living cells, strong electric fields are used. The electric stresses induce pores in the cell membrane, through which the molecules enter the cell. Ideally, these pores should reseal after the field is turned off. However, often the membrane collapses leading to cell death.

The physical mechanisms of membrane destabilization in electric fields remain poorly understood (Teissie, Golzio & Rols 2005). Theoretical models based on stability analyses have mainly focused on thickness fluctuations (Weaver & Chizmadzhev 1996). However, recent works have shown that bending modes can also destabilize the membrane, even at lower voltages (Sens & Isambert 2002; Lacoste, Lagomarsino & Joanny 2007; Schwalbe, Vlahovska & Miksis 2011). Experimental studies using giant vesicles (artificial cell-size membrane envelopes) have revealed that membrane deformation and poration depend crucially on the electric pulse duration (Riske & Dimova 2005; Dimova *et al.* 2009): a vesicle subjected to a long, weak pulse bursts while a vesicle subjected to a short, strong pulse survives (Salipante, Dimova & Vlahovska, unpublished observations).

† Email address for correspondence: petia_vlahovska@brown.edu

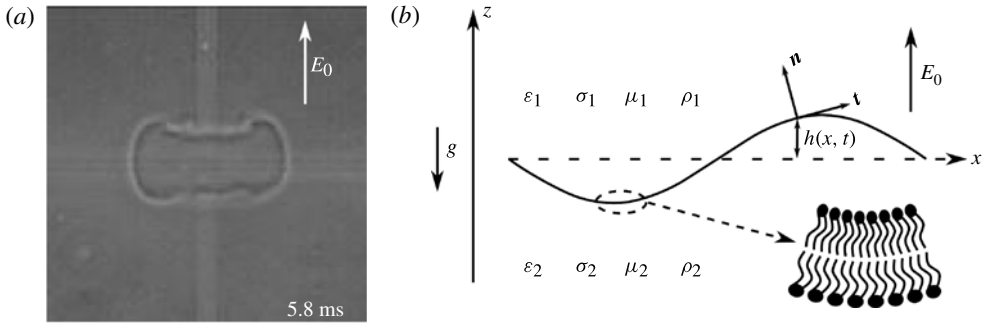

FIGURE 1. (*a*) Vesicle collapsing in a DC electric field (Salipante *et al.* unpublished observations). Leakage through pores causes loss of phase contrast and the interfaces facing the poles appear fuzzy. (*b*) A freely floating planar lipid bilayer membrane separating fluids with different physical and electrical properties is subjected to an uniform electric field E_0. The time-dependent displacement of the membrane above the x–y plane along the z-direction is $h(x, y, t)$.

The dynamics of fluid–fluid interfaces, e.g. water–air, stressed by a perpendicularly applied electric field, as sketched in figure 1, has been extensively studied since the pioneering work of Taylor & McEwan (1965). They found that the interface between conducting and non-conducting fluids ($\sigma_2 \gg \sigma_1$) is unstable when the applied electric field strength exceeds $E_c^2 = 2\gamma k_T/\varepsilon_1$, where $k_T = 2\pi\,[g(\rho_2 - \rho_1)/\gamma]^{1/2}$; here γ is the surface tension, $\rho_{1,2}$ are the fluid densities and g is the gravitational acceleration. Notably, if the fluids are density matched, i.e. $\rho_1 = \rho_2$, there is no threshold electric field. A follow-up study by Melcher & Smith (1969) highlighted the importance of the finite charge relaxation time. More recently, the discovery that thin polymer films form periodic arrays of pillars when subjected to a vertical DC (Schaffer *et al.* 2000; Pease & Russel 2002; Thaokar & Kumaran 2005; Wu & Russel 2009) or AC electric field (Roberts & Kumar 2009; Gambhire & Thaokar 2010) renewed interest in the electrohydrodynamic instabilities of fluid interfaces.

The main structural component of biomembranes is a lipid bilayer with typical thickness of ∼5 nm. The lipid molecules are free to move within a monolayer, and thus on scales larger than the bilayer thickness the membrane can be treated as two-dimensional fluid. However, bilayer membranes differ from ordinary fluid–fluid interfaces in several aspects. First, the finite bilayer thickness imparts resistance to changes in curvature. Second, the energy required for bending is comparable to the thermal energy, and thermally excited shape fluctuations are strong and visible with optical microscopy. Third, the number of lipid molecules in the bilayer is fixed and thus the interfacial area cannot change: the two-dimensional fluid is incompressible, and the membrane tension γ is not a material property but an adjustable parameter enforcing constant surface area (Seifert 1995).

Elastic properties of fluid membranes are described by the classic Helfrich energy (Helfrich 1973)

$$\mathscr{F} = \int \left[\frac{\kappa}{2}\,(2H)^2 + \gamma\right] \mathrm{d}A, \tag{1.1}$$

where κ is the bending modulus and H is the mean curvature. Equilibrium shape fluctuations with wavenumber q of a planar membrane embedded in a fluid with

viscosity μ are stable with relaxation rate $s(q) = -(\kappa q^3 + \gamma q)/4\mu$ (Brochard & Lennon 1975; Seifert & Langer 1993).

Electric fields affect the membrane undulations (Sens & Isambert 2002, Lacoste *et al.* 2007, 2009, Ziebert, Bazant & Lacoste 2010 and Ziebert & Lacoste 2010; recently reviewed in Ziebert & Lacoste 2011). Sens & Isambert (2002) highlighted that the electric field induces a negative tension in the membrane $\gamma_m \sim E_0^2$. An instability occurs above a threshold electric field at which the negative tension exceeds the initial tension in the membrane. Another source of instability found by Lacoste *et al.* (2007) is ion currents in the diffuse layers near the membrane, which give rise to a positive q^2 term in the relaxation rate. In the limit of zero Debye thickness this term vanishes, and the negative tension remains as the sole possible source for instability.

All these analyses have focused on a membrane separating fluids with the same permittivity and conductivity. Schwalbe *et al.* (2011) discovered that asymmetry in the electric properties of the embedding solutions, in particular difference in the conductivities $\sigma_1 \neq \sigma_2$, gives rise to an instability with no threshold electric field. Application of an electric field leads to the accumulation of ions (carried by conduction) at the membrane physical surfaces. The membrane acts as a (leaky) capacitor, whose charging is described by

$$C_m \frac{\mathrm{d}V_m}{\mathrm{d}t} + G_m V_m = \boldsymbol{n} \cdot (\sigma_1 \boldsymbol{E}_1) = \boldsymbol{n} \cdot (\sigma_2 \boldsymbol{E}_2), \tag{1.2}$$

where V_m is the potential jump across the membrane (transmembrane potential), C_m is the membrane capacitance, G_m is the membrane conductance due to pores, ion channels or pumps, and $\boldsymbol{J} = \sigma \boldsymbol{E}$ are the bulk ohmic currents. Schwalbe *et al.* (2011) investigated the dynamics of an insulating membrane ($G_m = 0$) and found that an instability can develop during the time over which the capacitor is charging, i.e. while capacitive charging current flows through the membrane. The model, however, ignored the effect of ohmic conduction current through the membrane. Experiments indicate that bilayer collapse is preceded by formation of nano-pores (Salipante *et al.* unpublished observations) (see figure 1*a*), which allow ions to pass through the membrane. Hence, the membrane conductivity may play an important role in the destabilization of the interface. In this paper, we investigate the interplay of capacitive charging and ohmic currents through the membrane in membrane dynamics and stability in DC electric fields.

2. Problem formulation

Let us consider a planar membrane formed by a charge-free lipid bilayer with dielectric constant ε_m and conductivity σ_m. The bilayer thickness d is ~5 nm, which is three orders of magnitude smaller than the radius of a typical cell. Accordingly, the membrane can be treated as a two-dimensional interface with effective capacitance $C_m = \varepsilon_m/d$ and conductance $G_m = \sigma_m/d$. The membrane separates a subphase fluid of conductivity σ_2, dielectric constant ε_2, viscosity μ_2, and density ρ_2 and superphase of a different fluid characterized by σ_1, ε_1, μ_1 and ρ_1. The membrane is subjected to an electric field created by a potential difference V applied across a distance $2L$. The problem is sketched in figure 1.

2.1. *Governing equations*

We adopt the leaky dielectric model, which combines the Stokes equations to describe fluid motion with conservation of current described by Ohm's law (Saville 1997).

The electric field is irrotational, $\boldsymbol{E}_k = -\boldsymbol{\nabla}\phi_k$, and the electric potential ϕ satisfies the Laplace equation

$$\nabla^2\phi_k = 0 \quad k = 1, 2, \tag{2.1}$$

where the top and bottom fluids are denoted by $k = 1$ and $k = 2$, respectively. The potential at the electrodes is $\phi_1(z = \pm L) = \mp V/2$. At the membrane interface $z = h(x, y, t)$, the potential is discontinuous $\phi_2 - \phi_1 = V_m$. The transmembrane potential V_m is determined from the conservation of normal current (see the Appendix for its derivation)

$$\boldsymbol{n} \cdot \left(\sigma_k \boldsymbol{E}_k + \varepsilon_k \frac{\partial \boldsymbol{E}_k}{\partial t}\right) + \nabla_s \cdot (\boldsymbol{v} Q_k) = C_m \frac{\partial V_m}{\partial t} + G_m V_m \quad (k = 1, 2), \tag{2.2}$$

which in the limit of fast bulk charge relaxation and negligible convection reduces to (1.2). Q_k are the induced charge densities on the top and bottom side of the membrane interface (A 2). The electric stress $\boldsymbol{\tau}_{el}$ acting on the membrane is then calculated from the Maxwell tensor

$$\boldsymbol{\tau}_{el} = \boldsymbol{n} \cdot (\boldsymbol{T}_1^{el} - \boldsymbol{T}_2^{el}), \quad \boldsymbol{T}_k^{el} = \varepsilon_k \left(\boldsymbol{E}_k \boldsymbol{E}_k - \tfrac{1}{2} \boldsymbol{E}_k \cdot \boldsymbol{E}_k \boldsymbol{I}\right). \tag{2.3}$$

In the context of biological membranes, inertia is negligible so that the velocity $\boldsymbol{v}$ and pressure p are solutions of the Stokes equations

$$\mu_k \nabla^2 \boldsymbol{v}_k = \boldsymbol{\nabla} p_k, \quad \boldsymbol{\nabla} \cdot \boldsymbol{v}_k = 0. \tag{2.4}$$

The no-slip boundary condition applies for the velocity field at the electrodes $\boldsymbol{v}(z = \pm L) = 0$. The area-incompressibility of the membrane implies that the surface velocity is solenoidal, $\nabla_s \cdot \boldsymbol{v}_s = 0$. The membrane moves with the normal velocity of the fluid due to the membrane impermeability on the time scale of interest. The fluid tractions $\boldsymbol{\tau}_{hd}$ on the membrane are inferred from the hydrodynamic stress tensor

$$\boldsymbol{\tau}_{hd} = \boldsymbol{n} \cdot (\boldsymbol{T}_1^{hd} - \boldsymbol{T}_2^{hd}), \qquad \boldsymbol{T}_k^{hd} = -p_k \boldsymbol{I} + \mu_k [\boldsymbol{\nabla} \boldsymbol{v}_k + (\boldsymbol{\nabla} \boldsymbol{v}_k)^{\mathrm{T}}], \tag{2.5}$$

where T denotes the transpose. The pressure, viscous, and electric stresses undergo a jump across the membrane, which is balanced by membrane elastic stresses derived from the Helfrich energy (1.1) (Seifert 1999)

$$\boldsymbol{\tau}_m = -\kappa [4H^3 - 4HK_G + 2\nabla_s^2 H]\boldsymbol{n} + 2\gamma H \boldsymbol{n} - \nabla_s \gamma, \tag{2.6}$$

where K_G is the Gaussian curvature. The last term in (2.6) arises under non-equilibrium conditions, in which the tension γ can become non-uniform in order to enforce the local area incompressibility. Finally the kinematic condition determines the location of the interface.

2.2. *Dimensionless parameters and rescaling*

Upon application of an electric field, bulk fluids become electroneutral on the charge relaxation time scales (Melcher & Taylor 1969)

$$t_1 = \frac{\varepsilon_1}{\sigma_1}, \quad t_2 = \frac{\varepsilon_2}{\sigma_2}. \tag{2.7}$$

The electrohydrodynamic flow which drives membrane bending is characterized by

$$t_{el} = \frac{\mu_1 + \mu_2}{\varepsilon_1 E_0^2}, \tag{2.8}$$

where $E_0 = V/2L$ is the characteristic magnitude of the imposed electric field. Resistance to changes in membrane curvature drives relaxation on a time scale

$$t_\kappa = \frac{\mu_1 + \mu_2}{\kappa l^3}, \tag{2.9}$$

where l is the curvature of the interface; for a membrane undulation with wavenumber q, $l \sim q$. An additional restoring mechanism is provided by the charging of the membrane capacitor, which acts to decrease the difference between the free charge densities on the two membrane surfaces. The smaller the surface charge imbalance, the weaker the destabilizing electric stresses; a fully charged membrane is stable to small disturbances (Schwalbe *et al.* 2011). For a purely capacitive membrane ($G_m = 0$), the capacitor time scale is

$$t_m = LC_m(\sigma_1^{-1} + \sigma_2^{-1}). \tag{2.10}$$

Henceforth, all quantities are rescaled by the properties of the top fluid; the distance between the membrane and the electrode L is the characteristic length scale, the time scale is LC_m/σ_1, the charge scale is $\varepsilon_1 E_0$, and stresses are scaled with $\varepsilon_1 E_0^2$. To analyse the problem systematically we introduce three dimensionless parameters:

$$Ca = \frac{t_\kappa}{t_{el}} = \frac{\epsilon_1 E_0^2 L^3}{\kappa}, \quad \alpha = \frac{t_1}{t_m} = \frac{\epsilon_1}{LC_m}, \quad \beta = \frac{\epsilon_1 E_0^2 C_m L}{\mu_1 \sigma_1} \approx \frac{t_m}{t_{el}}, \tag{2.11}$$

where α controls the importance of charge relaxation. β and the capillary number Ca compare capacitive and elastic effects to electrohydrodynamics; it is expected that higher values of these two parameters correspond to more unstable configurations.

Four additional parameters describe the physical properties of the system: $R = \sigma_2/\sigma_1$ and $S = \varepsilon_2/\varepsilon_1$, which measure the electrical mismatch between the two fluids, the viscosity ratio $\lambda = \mu_2/\mu_1$, and the non-dimensional membrane conductance $g_m = G_m L/\sigma_1$.

3. Problem solution

Here we perform a linear stability analysis by studying the dynamics of a shape fluctuation mode $h(x, t) = h_q \mathrm{e}^{st+\mathrm{i}qx}$. Without loss of generality we consider only a wave vector parallel to the x-axis. Accordingly, any variable u is expanded in a series of the form $u = u^{(0)}(z, t) + u^{(1)}(z, x, t) + \cdots$. The superscript (0) corresponds to the base state, $h = 0$; $u^{(1)} = u_q(z)\exp(st + \mathrm{i}qx)$ is a linear correction accounting for the effect of the small undulations.

In the base state of the system, where the membrane is flat and located at $z = 0$, the electric field is uniform in the bulk, $\boldsymbol{E}_k^{(0)} = E_k^{(0)}\hat{\boldsymbol{z}}$, and at the steady state (fully charged capacitor, $\partial_t V_m = 0$)

$$E_2^{(0)} = R^{-1}E_1^{(0)} = \delta, \quad \delta = \frac{g_m}{R + g_m(1 + R)}. \tag{3.1}$$

The potential is discontinuous across the membrane, $V_m = \phi_2(0) - \phi_1(0) = \delta R/g_m$. The limit $g_m \to \infty$ formally recovers the solution for a 'simple' fluid–fluid interface, which is characterized by a continuous potential. A flat interface experiences only electric pressure:

$$p^{el,(0)} = \tfrac{1}{2}[(E_1^{(0)})^2 - S(E_2^{(0)})^2] = \delta^2(R^2 - S). \tag{3.2}$$

The electric field $\boldsymbol{E}^{(0)}$ does not generate shear tractions, and the tension γ is uniform at leading order. Since the electric pressure is isotropic it follows that $\boldsymbol{v}^{(0)} = 0$, i.e. the system is in hydrostatic equilibrium.

The governing equations in § 2.1 can now be linearized about the base state (Schwalbe 2010; Ziebert & Lacoste 2011), resulting in

$$sh_q = \beta f(q)(p^{(1)}_{el,q} - F(q)h_q), \tag{3.3}$$

where

$$F(q) = Ca^{-1}(q^4 + \gamma q^2) + B, \quad f(q) = \frac{\cosh 2q - 1 - 2q^2}{2(1+\lambda)q(2q + \sinh 2q)}. \tag{3.4}$$

$F(q)$ describes the restoring effects of membrane elastic stresses (from (2.6)) and gravity, $B = (\rho_2 - \rho_1)gL/\varepsilon_1 E_0^2$.

In the absence of an electric field, (3.3) reduces to the classic result of Brochard & Lennon (1975) for an unbounded, tensionless, symmetric membrane ($\mu_1 = \mu_2, \rho_1 = \rho_2$), $s = -\kappa q^3/4\mu_1, q^{-1} \ll L$ (written in dimensional form). In the opposite limit of a wall-bounded membrane, $q^{-1} \gg L$, we find $s = -\kappa L^3 q^6/12\mu_1$ in agreement with Prost, Manneville & Bruinsma (1998).

The electric field effect on the growth rate s depends on the sign of the perturbation in the electric pressure:

$$p^{el,(1)} = E^{(0)}_{z,1}E^{(1)}_{z,1} - S(E^{(0)}_{z,2}E^{(1)}_{z,2}). \tag{3.5}$$

The above equation shows that the electric stress in the perturbed state depends crucially on the bulk electric field in the base state. If $\boldsymbol{E}^{(0)}$ is zero, then the electric stress, which is linear in the perturbation, vanishes and the membrane is linearly stable.

The electric field also generates tangential tractions. In the case of a simple fluid–fluid interface (characterized by constant surface tension) this creates tangential surface flow. In the case of a bilayer membrane, however, surface-incompressibility, $\nabla_s \cdot \boldsymbol{v}_s = 0$, dictates that the tangential component of the velocity $v_x^{(1)} = 0$. The electric shear stresses are balanced by gradients in the membrane tension. The tension varies as $\gamma^{(1)} = \gamma_0 + \gamma_q e^{st+iqx}$, and γ_q is determined from the tangential stress balance.

To find the electric pressure, we solve for the electric potential

$$\phi^{(1)}_{1q} = A_{1q}\exp(-qz), \quad \phi^{(1)}_{2q} = A_{2q}\exp(qz), \tag{3.6}$$

where A_{1q} and A_{2q} are determined from the two current conservation conditions (2.2):

$$A_{2q}(R + s\alpha S) = -A_{1q}(1 + \alpha s), \tag{3.7}$$

$$qA_{1q}(1 + \alpha s) = (s + g_m)(A_{2q} - A_{1q} + h_q E^{(0)}_2(R - 1)). \tag{3.8}$$

From (3.5) we obtain for the normal electric stress

$$p^{(1)}_{el,q} = qE^{(0)}_2(RA_{1q} + SA_{2q}). \tag{3.9}$$

Thus the dispersion relation (3.3) becomes

$$c_3 s^3 + c_2 s^2 + c_1 s + c_0 = 0, \tag{3.10}$$

where

$$c_0 = \beta f(q)[qRF(q) - g_m(\delta^2 q(R-1)(R^2 - S) + (R+1)F(q))], \tag{3.11a}$$

$$c_1 = g_m(R+1) + qR + \beta f(q)[g_m\alpha((S+1)F(q) - \delta^2 q\,(R-1)^2\,S) + F(q)(R+1) + q\alpha(R+S) + \delta^2 q(R-1)(R^2 - S)], \tag{3.11b}$$

$$c_2 = R + 1 + g_m\alpha(S+1) + q\alpha(R+S) + \alpha\beta f(q)[-\delta^2 q\,(R-1)^2\,S + (S+1+q\alpha S)F(q)], \tag{3.11c}$$

$$c_3 = \alpha(1+S+\alpha q S). \tag{3.11d}$$

In the limit of an unbounded membrane, $L \to \infty$, and instantaneous charge relaxation $\alpha = 0$, the growth rate of a tension-free membrane separating density matched fluids ($\gamma = 0, B = 0$) in dimensional form becomes

$$s_{L\to\infty} = t_{el}^{-1}\frac{(R-1)(R^2-S)}{(R+1)^2(1+R+Rq\sigma_1/G_m)} - \frac{\kappa q^3}{2\mu_1(1+\lambda)}. \tag{3.12}$$

The above expression generalizes the Brochard & Lennon (1975) result for the fluctuations of a tensionless, symmetric membrane in the presence of electric field. Interestingly, long wavelength undulations with $q(1+R)\sigma_1/G_m \ll 1$ are insensitive to the membrane conductivity. For an insulating membrane, $g_m = 0$ (and thus $\delta = 0$), the solutions of (3.10) for the growth rate are always negative, $s = -\beta f(q)F(q), -1/\alpha, -R/S\alpha$, and the membrane is stable. This is in contrast to a simple fluid–fluid interface, where charge relaxation ($\alpha > 0$) can lead to instability (Melcher & Smith 1969). In general, (3.10) has three solutions, which can be real or complex. The growth rate s of a given perturbation is the largest real part of these. The complexity of the dispersion equation suggests we explore some less involved limiting cases.

4. Results

In electrodeformation experiments with cells or giant lipid vesicles, the fluids are aqueous salt solutions. Therefore, our analysis focuses on the case of equal-density and equal-viscosity fluids, $\rho_1 = \rho_2$ and $\mu_1 = \mu_2 \approx 10^{-3}$ Pa s. Typical values for the other physical variables are $\sigma \sim 10^{-6}$–10^{-3} S m^{-1}, $C_m \sim 0.01$ F m^{-2}, $L \sim 100$ μm, $\kappa \sim 10^{-19}$ J, $E_0 \sim 1$ kV m^{-1} (Dimova *et al.* 2007, 2009; Salipante *et al.* 2012). It is difficult to pick a typical value for g_m as it varies by orders of magnitude; indeed the conductivity of an intact membrane is very low ($\sim 10^{-12}$ S m^{-1}), but can approach that of the surrounding liquid when it opens pores (DeBruin & Krassowska 1999). Thus $G_m \sim 10^{-3}$–10^{6} S m^{-2}.

These data show that the conductivity ratio can vary over a broad range $R \sim 10^{-3}$–10^{3}, whereas the permittivity ratio S is of order one. Typical values for the other dimensionless numbers are $Ca \sim 10^5$, $g_m \sim 10^{-4}$–10^{8} ($g_m \sim 10^{-4}$–10^{-1} without membrane poration), $\alpha \sim 10^{-4}$–10^{-1} and $\beta \sim 10^{-3}$–1. The low values of α suggest that usually charge relaxation is faster than the capacitor charging.

We also discuss only the bending as a restoring force because it is a unique feature of bilayer membranes, i.e. $F(q) = -Ca^{-1}q^4$. The effects of gravity can be explored in a straightforward manner using the complete form of the restoring function, (3.4). The effects of tension are more subtle. The tension of a fluctuating membrane in the absence of an electric field is very low $\gamma_0 \sim 10^{-6}$ N m^{-1} (Evans & Rawicz 1990; Kummrow & Helfrich 1991). The electric field has a two-fold effect on the tension. On one side, the finite-thickness membrane experiences a compressive electric stress, which effectively decreases the isotropic tension (Needham & Hochmuth 1989; Ziebert & Lacoste 2011), $\gamma = \gamma_0 - \varepsilon_m V_m^2/d$. On the other side, the electric pressure acts to straighten the undulations (recorded as vesicle deformation in experiments Kummrow & Helfrich 1991), which raises the tension. We leave the more detailed study of the

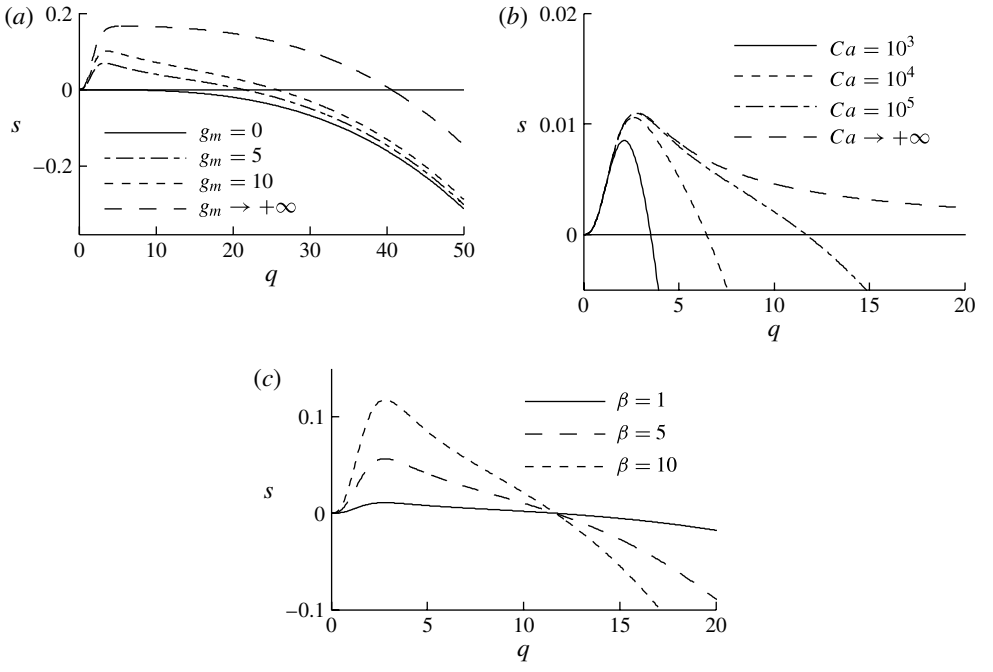

FIGURE 2. The effect of (*a*) g_m, (*b*) Ca, (*c*) β on growth rate s as a function of perturbation wavenumber q, for $R = 10$, $S = 1$, $\alpha = 0$. (*a*) $Ca = 10^5$, $\beta = 1$; (*b*) $g_m = 1$, $\beta = 1$; (*c*) $g_m = 1$, $Ca = 10^5$.

effects of tension to a future study and here we centre our attention on the case of a freely floating membrane, which is tensionless in its base state $\gamma_0 = 0$.

4.1. *Instantaneous charge relaxation* ($\alpha = 0$)

Setting $\alpha = 0$ reduces the dispersion relation (3.10) to a quadratic equation, whose complex solutions have no positive real part. This greatly simplifies the analysis, since every unstable solution must then be real, and it cannot be positive if all the coefficients of the polynomial equation are positive, that is, if $g_m(R-1)(R^2-S) \leqslant 0$. In the opposite case, as shown in figure 2, the membrane can become unstable for long waves.

A closer inspection of the behaviour of the dispersion relation near the origin, $q \to 0$, shows that it simplifies to

$$s_{q\to+0} = \beta q^3 \frac{g_m^2(R-1)(R^2-S)}{24\,(R+g_m(1+R))^2} + O(q^4). \tag{4.1}$$

Equation (4.1) indicates that an unstable domain must exist near $q = 0$ when $g_m > 0$ and $(R-1)(R^2-S) > 0$. The membrane is thus always unstable if the fluids have very different conductivities, that is, $R \ll 1$ or $R \gg 1$, but it may become stable for intermediate values of R. This conclusion is illustrated in figure 3, where the maximal growth rate s_{max} is plotted as a function of R, for different values of S. In this logarithmic plot, curves are only shown if $s_{max} > 0$, i.e. if the system is unstable.

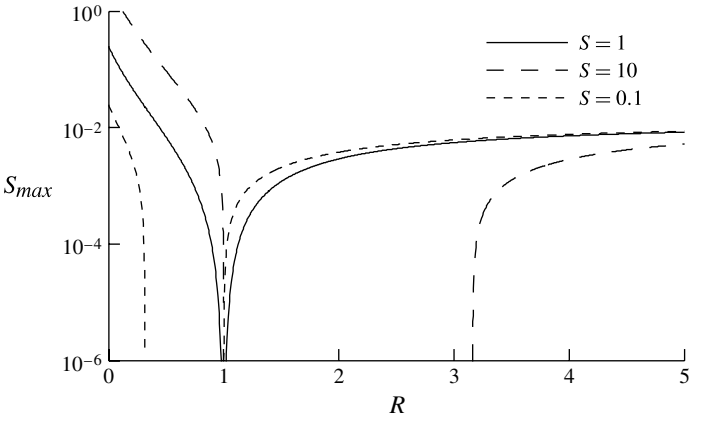

FIGURE 3. Maximal growth rate s_{max} as function of R, for $g_m = 1$, $Ca = 10^5$, $\beta = 1$, $\alpha = 0$ and different values of S. In this semi-logarithmic plot, each curve only exists where the system is unstable, that is, for $(R-1)(R^2-S) > 0$. When $S > 1$, for example (long-dashed line), the membrane is unstable when $R < 1$ or $R > \sqrt{S}$.

The wavenumber q_c corresponding to marginal stability $s = 0$, excluding the trivial solution $q_c = 0$, is a solution of a simple quartic equation:

$$Ca^{-1} q_c^3 (q_c R + g_m(1+R)) = \left(E_2^{(0)}\right)^2 g_m (R-1)(R^2-S). \tag{4.2}$$

Equation (4.2) allows us to recover the criterion of instability previously derived: a strictly positive solution exists (i.e. the system is unstable in a finite window of wavenumbers) if and only if $g_m(R-1)(R^2-S) > 0$. Moreover, there is only one unstable region $0 < q < q_c$. Lastly, q_c does not depend on β.

Next we discuss the dependence of the instability on g_m, Ca and β. Figure 2(*a*) shows that the membrane conductivity enhances the instability. Increasing g_m decreases the effect of the membrane capacitance and when $g_m \to +\infty$ the capacitor is totally short-circuited. In experiments, vesicles or cells are likely to be in this limit as soon as they porate. The growth rate tends towards a limit value which satisfies the following equation:

$$s_{g_m \to +\infty} = \beta f(q) \left[q \frac{(R-1)(R^2-S)}{(R+1)^3} - Ca^{-1} q^4 \right]. \tag{4.3}$$

Equation (4.3) illustrates the two antagonist phenomena: the electric pressure that is destabilizing if $(R-1)(R^2-S) > 0$, and the stabilizing bending stresses. In the limit $g_m \to +\infty$ the transmembrane potential vanishes, and from an electrical standpoint, the membrane acts as a simple fluid–fluid interface. Thus, figure 2(*a*) suggests that a simple fluid interface is more unstable than the capacitive membrane. Mechanically, however, the membrane differs from a simple interface, since the membrane is surface-incompressible. Thus, only a qualitative comparison with published results on fluid–fluid interface stability is possible.

The effect of the applied voltage is illustrated in figure 2(*b*). The growth rate monotonically increases with Ca, reaching an asymptotic value at $Ca \to +\infty$ (i.e. vanishing membrane rigidity), found by formally setting $Ca^{-1} = 0$ in (3.10). In this limit, all wavelengths are unstable. Mathematically, this comes from the fact that the $Ca^{-1} \sim 0$ assumption is only valid for $q \ll Ca^{1/3}$, but more interestingly it

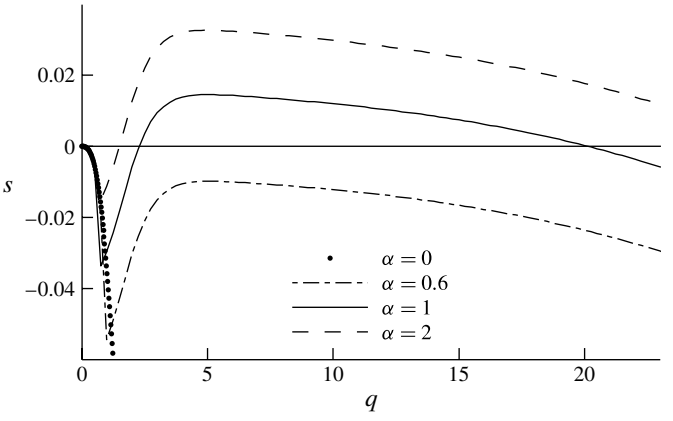

FIGURE 4. Growth rate s as a function of q for $g_m = 100$, $Ca = 10^5$, $R = 5$, $\beta = 1$ and $S = 80$. When $\alpha = 0$ (dashed line), the system is always stable as $(R-1)(R^2-S) < 0$. When $\alpha = 1$, an unstable region appears at shorter wavelengths.

shows that the largest unstable wavenumber q_c diverges as $Ca \to +\infty$. There is no threshold voltage for the instability to occur, in agreement with the finding by Taylor & McEwan (1965) for an interface separating fluids with the same density. The applied voltage is also included in β, which characterizes the mismatch between the electrohydrodynamic and capacitor charging time scales. Figure 2(*c*) shows that β enhances the instability: the faster the electrohydrodynamic time compared to the capacitor charging time, the higher the maximum growth rate. However, the window of unstable wavenumbers and the most unstable mode remain unchanged. Note that s_{max} increases linearly with β, see (4.3).

4.2. *Effect of charge relaxation* $\alpha > 0$

Until now we have assumed $\alpha = 0$, which is a good approximation in usual experiments. However, formally setting $\alpha = 0$ is justified only when $\alpha|s| \ll 1$. We could then expect a qualitative difference at large growth rates, even when $\alpha \ll 1$. This happens when $\beta \to +\infty$ (because s increases with β) or $q \to +\infty$, although the latter case is usually considered less interesting since the growth rate is large but negative, and the system is stable. However, as shown in figure 4, a window of unstable large wavenumbers can appear. Thus, the previous instability criterion $g_m(R-1)(R^2-S) > 0$ no longer holds when $\alpha > 0$, although it still governs the behaviour of s near $q = 0$. The values of the parameters needed for this unexpected instability are somewhat different from those chosen in the context of biological experiments, but they are well within experimental reach. In particular, the value $S = 80$ used in figure 4 corresponds to an air–water interface. Admittedly, in this case one has to account for the density difference between the two fluids. However, gravity stabilizes only long wavelengths and does not affect the observed range of unstable short wavelength undulations

5. Conclusions and outlook

We have developed a physical model for the dynamic coupling between transmembrane potential (induced by an applied uniform electric field) and deformation of biomimetic membranes. We perform linear stability analysis to clarify and quantify the effects of the lipid bilayer properties (conductivity and capacitance),

and asymmetry in the embedding electrolyte solutions, on membrane dynamics. Previous work on non-conducting membranes by Schwalbe *et al.* (2011) found only a transient instability upon application of the electric field. Our study shows that in a steady DC electric field, in contrast to the purely capacitive membrane, a conducting membrane is unstable to long-wavelength perturbations if the fluids have different conductivities $g_m(R-1)(R^2-S)>0$. In the considered case of density-matched fluids, there is no threshold voltage for the instability. An interesting new result is that finite charge relaxation can open another instability window at shorter wavelengths.

The developed theory applies only to small perturbations in shape and linear ohmic conductance of the membrane. The experiments on collapsing vesicles shown in figure 1(*a*) involve large membrane deformations, which can be explored by a nonlinear stability analysis based on lubrication theory or numerical simulation. Biological membranes typically possess nonlinear conductance. In this case, Leonetti, Dubois-Violette & Homble (2004) found an intriguing electrodiffusive instability which can lead to patterns in the membrane potential. However, in their study membrane deformation was not considered. We hope our work will stimulate further research on the electrohydrodynamics of deformable bio-membranes.

Acknowledgements

P.M.V. acknowledges partial financial support by NSF grant CBET-1117099. M.J.M. acknowledges financial support by NSF grant DMS- 0616468.

Appendix. Current conservation

To include charge convection by fluid motion and time-dependent charge build-up, we need to consider the charge conservation at the two physical surfaces

$$\boldsymbol{n}\cdot(\boldsymbol{J}_1-\boldsymbol{J}_m)=-\frac{\partial Q_1}{\partial t}-\nabla_s\cdot(\boldsymbol{v}Q_1)\quad z=0^+, \tag{A 1a}$$

$$\boldsymbol{n}\cdot(\boldsymbol{J}_m-\boldsymbol{J}_2)=-\frac{\partial Q_2}{\partial t}-\nabla_s\cdot(\boldsymbol{v}Q_2)\quad z=0^-. \tag{A 1b}$$

Here $\nabla_s=\boldsymbol{I}_s\cdot\nabla$ is the surface gradient operator and $\boldsymbol{I}_s=\boldsymbol{I}-\boldsymbol{nn}$ is the surface projection. The charge density on the top, Q_1, and bottom, Q_2, side of the membrane interface are

$$Q_1=\boldsymbol{n}\cdot(\varepsilon_1\boldsymbol{E}_1)-C_mV_m,\quad Q_2=C_mV_m-\boldsymbol{n}\cdot(\varepsilon_2\boldsymbol{E}_2), \tag{A 2}$$

where for a thin membrane we use the approximation $\varepsilon_m\boldsymbol{n}\cdot\boldsymbol{E}_m=C_mV_m$.

The classic leaky dielectric model for a 'simple' interface developed by G. I. Taylor is recovered by writing the surface charge as $Q=Q_1+Q_2$, and adding the two transport equations, (A 1), on the top and bottom interface. Noting that the ohmic current through the membrane $\boldsymbol{J}_m=\sigma_m\boldsymbol{E}_m$, and charge convection is negligible (at leading order the tangential surface velocity is zero due to membrane area–incompressibility), (A 1) can be rewritten as (2.2).

REFERENCES

BROCHARD, F. & LENNON, J. F. 1975 Frequency spectrum of the flicker phenomenon in erythrocytes. *J. Phys. (France)* **36**, 1035–1047.

DEBRUIN, K. & KRASSOWSKA, W. 1999 Modeling electroporation in a single cell. Part 1. Effects of field strength and rest potential. *Biophys. J.* **77**, 1213–1224.

DIMOVA, R., BEZLYEPKINA, N., JORDO, M. D., KNORR, R. L., RISKE, K. A., STAYKOVA, M., VLAHOVSKA, P. M., YAMAMOTO, T., YANG, P. & LIPOWSKY, R. 2009 Vesicles in electric fields: some novel aspects of membrane behaviour. *Soft Matt.* **5**, 3201–3212.

DIMOVA, R., RISKE, K. A., ARANDA, S., BEZLYEPKINA, N., KNORR, R. L. & LIPOWSKY, R. 2007 Giant vesicles in electric fields. *Soft Matt.* **3**, 817–827.

EVANS, E. & RAWICZ, W. 1990 Entropy driven tension and bending elasticity in condensed-fluid membranes. *Phys. Rev. Lett.* **64**, 2094–2097.

GAMBHIRE, P. & THAOKAR, R. M. 2010 Electrohydrodynamic instabilities at interfaces subjected to alternating electric field. *Phys. Fluids* **22**, 064103.

HELFRICH, W. 1973 Elastic properties of lipid bilayers: theory and possible experiments. *Z. Naturforsch.* **28c**, 693–703.

KUMMROW, M. & HELFRICH, W. 1991 Deformation of giant lipid vesicles by electric fields. *Phys. Rev.* A **44**, 8356–8360.

LACOSTE, D., LAGOMARSINO, M. C. & JOANNY, J. F. 2007 Fluctuations of a driven membrane in an electrolyte. *Europhys. Lett.* **77**, 18006.

LACOSTE, D., MENON, G. I., BAZANT, M. Z. & JOANNY, J. F. 2009 Electrostatic and electrokinetic contributions to the elastic moduli of a driven membrane. *Eur. Phys. J.* E **28**, 243–264.

LEONETTI, M., DUBOIS-VIOLETTE, E. & HOMBLE, F. 2004 Pattern formation of stationary transcellular ionic currents in Fucus. *PNAS* **101**, 10243–10248.

MELCHER, J. R. & SMITH, C. 1969 Electrohydrodynamic charge relaxation and interfacial perpendicular-field instability. *Phys. Fluids* **12**, 778–790.

MELCHER, J. R. & TAYLOR, G. I. 1969 Electrohydrodynamics: a review of role of interfacial shear stress. *Annu. Rev. Fluid Mech.* **1**, 111–146.

NEEDHAM, D. & HOCHMUTH, R. M. 1989 Electromechanical permeabilization of lipid vesicles. role of membrane tension and compressibility. *Biophys. J.* **55**, 1001–1009.

PEASE, L. F. & RUSSEL, W. B. 2002 Linear stability analysis of thin leaky dielectric films subjected to electric fields. *J. Non-Newtonian Fluid Mech.* **102**, 233–250.

PROST, J., MANNEVILLE, J.-B. & BRUINSMA, R. 1998 Fluctuation-magnification of non-equilibrium membranes near a wall. *Eur. Phys. J.* B **1**, 465–480.

RISKE, K. A. & DIMOVA, R. 2005 Electro-deformation and poration of giant vesicles viewed with high temporal resolution. *Biophys. J.* **88**, 1143–1155.

ROBERTS, S. A. & KUMAR, S. 2009 AC electrohydrodynamic instabilities in thin liquid films. *J. Fluid Mech.* **631**, 255–279.

SALIPANTE, P. F., KNORR, R., DIMOVA, R. & VLAHOVSKA, P. M. 2012 Electrodeformation method for measuring the capacitance of bilayer membranes. *Soft Matt.* **8**, 3810–3816.

SAVILLE, D. A. 1997 Electrohydrodynamics: the Taylor–Melcher leaky dielectric model. *Annu. Rev. Fluid Mech.* **29**, 27–64.

SCHAFFER, E., THURN-ALBRECHT, T., RUSSELL, T. & STEINER, U. 2000 Electrically induced structure formation and pattern transfer. *Nature* **603**, 874–877.

SCHWALBE, J. 2010 Dynamics and stability of lipid bilayer membranes in viscous flow and electric fields. PhD thesis, Northwestern University.

SCHWALBE, J. T., VLAHOVSKA, P. M. & MIKSIS, M. J. 2011 Lipid membrane instability driven by capacitive charging. *Phys. Fluids* **23**, 04170.

SEIFERT, U. 1995 The concept of effective tension for fluctuating vesicles. *Z. Phys.* B **97**, 299–309.

SEIFERT, U. 1999 Fluid membranes in hydrodynamic flow fields: formalism and an application to fluctuating quasispherical vesicles. *Eur. Phys. J.* B **8**, 405–415.

SEIFERT, U. & LANGER, S. 1993 Viscous modes of fluid bilayer membranes. *Europhys. Lett.* **23**, 71–76.

SENS, P. & ISAMBERT, H. 2002 Undulation instability of lipid membranes under an electric field. *Phys. Rev. Lett.* **88**, 128102.

TAYLOR, G. I. & MCEWAN, A. D. 1965 The stability of a horizontal fluid interface in a vertical electric field. *J. Fluid Mech.* **22**, 1–15.

TEISSIE, J., GOLZIO, M. & ROLS, M. P. 2005 Mechanisms of cell membrane electropermeabilization: a minireview of our present (lack of ?) knowledge. *Biochimica et Biophysica Acta (BBA): General* **1724**, 270–280.

THAOKAR, R. M. & KUMARAN, V. 2005 Electrohydrodynamic instability of the interface between two fluids confined in a channel. *Phys. Fluids* **17**, 084104.

WEAVER, J. C. & CHIZMADZHEV, Y. A. 1996 Theory of electroporation: a review. *Bioelectrochem. Bioenerg* **41**, 135–160.

WU, N. & RUSSEL, W. B. 2009 Micro- and nano-patterns created via electrohydrodynamic instabilities. *Nanotoday* **4**, 180.

ZIEBERT, F., BAZANT, M. Z. & LACOSTE, D. 2010 Effective zero-thickness model for a conductive membrane driven by an electric field. *Phys. Rev.* E **81**, 031912.

ZIEBERT, F. & LACOSTE, D. 2010 A Poisson–Boltzmann approach for a lipid membrane in an electric field. *New J. Phys.* **12**, 095002.

ZIEBERT, F. & LACOSTE, D. 2011 A planar lipid bilayer in an electric field: membrane instability flow field, and electrical impedance. In *Advances in Planar Lipid Bilayers and Liposomes* (ed. A. Iglic), vol. 14, pp. 63, 95. Elsevier.